*Inorg. Chem.* **2007**, *46*, 7154–7162

# Preparation and Structure of Three Solvatomorphs of the Polymer $[Co(dbm)_2(4ptz)]_n$: Spin Canting Depending on the Supramolecular Organization

**Leoní A. Barrios, Joan Ribas, and Guillem Aromí***

*Universitat de Barcelona, Departament de Química Inorgànica, Diagonal 647, 08028 Barcelona, Spain*

**Jordi Ribas-Ariño**

*Universitat de Barcelona, Departament de Química Física and CERQT, Diagonal 647, 08028 Barcelona, Spain*

**Patrick Gamez**

*Leiden Institute of Chemistry, Gorlaeus Laboratories, Leiden University, P. O. Box 9502, 2300 RA Leiden, The Netherlands*

**Olivier Roubeau**

*Université de Bordeaux − CNRS CRPP, 115 av. Dr A. Schweitzer, 33600 Pessac, France*

**Simon J. Teat**

*CCLRC Daresbury Laboratory, Warrington, Cheshire, UK WA4 4AD and Advance Light Source, Lawrence Berkeley Lab, 1 Cyclotron Rd, MS2-400, Berkeley, California 94720*

Received March 14, 2007

The syntheses and X-ray structures of three isomeric 1D coordination polymers are reported. The complex $[Co(dbm)_2(MeOH)_2]$ (**1**) was used as a precursor in these reactions. The preparation and structure of **1** is also presented; this mononuclear complex is in the cis configuration because this allows the formation of a network of intermolecular hydrogen bonds in the solid state. Reaction of **1** with 2,4,6-tris-(4-pyridyl)-1,3,5-triazine (4ptz) yields the polymers $[Co(dbm)_2(4ptz)]_n \cdot n$THF (**2a**), $[Co(dbm)_2(4ptz)]_n \cdot 0.75n$THF$\cdot 0.5n$Et$_2$O (**2b**), and $[Co(dbm)_2(4ptz)]_n \cdot 3n$DMF (**2c**) in the form of zigzag chains, instead of the expected honeycomb architectures. This is because of the establishment of extended $\pi$–$\pi$ stacking throughout these solids, which could not have occurred otherwise. Compounds **2a**, **2b**, and **2c** are solvatomorphs, and formation of either one of them depends on the exact conditions of crystallization, which lead to significant differences in the supramolecular organization of the chains. Bulk magnetic measurements on **2a** reveal weak antiferromagnetic exchange within the chains and small ordering throughout the solid that results in the manifestation of the phenomenon of spin canting, whereas for **2c** the different supramolecular organization causes the antiferromagnetic exchange not to result in spin canting.

## Introduction

Self-assembly has been defined as *"the process by which specific components spontaneously assemble in a highly selective fashion into a well-defined, discrete supramolecular architecture"*.[1] Since the mid-1990s, research in coordination chemistry has been influenced strongly by the development of metallo-supramolecular chemistry,[2] which involves the design and preparation of intricate polymetallic coordination

* To whom correspondence should be addressed. E-mail: guillem.aromi@qi.ub.es.

(1) Lehn, J.-M. *Supramolecular Chemistry*; VCH Publishers: New York, 1995.
(2) Steel, P. J. *Acc. Chem. Res.* **2005**, *38*, 243−250.



10.1021/ic7004979 CCC: $37.00 
Published on Web 07/27/2007

**Scheme 1.** 4ptz Ligand

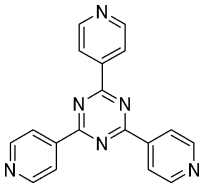

aggregates with specific structures or functions.[3] Along these lines, the creation of supramolecular networks can be accomplished by the judicious combinations of organic ligands and metals,[4] thus exploiting the ability of metal−ligand coordination bonds to provide simple and controlled routes to 1D, 2D, or 3D metal−organic frameworks (MOFs),[5] which constitute an exotic class of coordination polymers and may exhibit unique properties.[6−8] The bottom-up assembly of MOFs from metal ions and organic linkers is among the cornerstones of crystal engineering. In this context, the final architecture might exhibit additional levels of supramolecular organization, by exploiting other weak interactions such as hydrogen bonding or $\pi-\pi$ interactions, among others. We have been interested in the preparation of novel MOFs with relevance in the area of molecular magnetism. One of our goals is that of organizing magnetic nodes within coordination polymers with predetermined structures in order to gain control of the magnetic properties of the final material.

For some time, we have been exploring the coordination chemistry of triazine-based ligands with various paramagnetic metals and have synthesized an important number of discrete or extended polynuclear arrays with unprecedented topologies and unusual magnetic properties.[9−11] We have now turned our attention to the trigonal ligand 2,4,6-tris-(4-pyridyl)-1,3,5-triazine (4ptz, Scheme 1) as a tridentate coordination node imposing a directionality of 120°. This ligand has been previously employed in the preparation of very interesting MOFs, involving non-paramagnetic metallic ions for the most part, aimed at fulfilling various roles such as host−guest functions.[12−15] The reactivity of 4ptz with simple complexes of cobalt(II), as possible 180° connecting nodes, was explored here in order to construct extended paramagnetic frameworks expected to form honeycomb arrangements. A requirement for such an organization is that the coordination positions of the metal, other than the axial ones, remain blocked by other co-ligands. This type of arrangement built from 4ptz has one precedent where the metallic linear links are formed by strongly antiferromagnetically coupled, thus quasi-diamagnetic, [Cu$_2$] acetate-bridged dimers.[16]

## Results and Discussion

**Synthesis.** To find a suitable source of octahedral cobalt(II) with four equatorial positions occupied by chelating ligands, and with two labile axial ligands, we decided to prepare complex [Co(dbm)$_2$(MeOH)$_2$] (**1**). This complex was thus expected to act as a linear building block within supramolecular arrangements where it would be incorporated by the coordination of external ligands at the axial positions, while keeping the equatorial plane saturated by the chelating dbm$^-$ donors. The mononuclear compound is not described in the literature, although the electrochemical synthesis of the corresponding EtOH analogue has been reported.[17] Complex **1** could be conveniently prepared from the very clean reaction (eq 1) of dibenzoylmethane (Hdbm) with Co(AcO)$_2$ in MeOH, from where the product precipitates in

$$\mathrm{Co(AcO)_2} + 2\mathrm{Hdbm} + 2\mathrm{MeOH} + [\mathrm{Co(dbm)_2(MeOH)_2}] + 2\mathrm{AcOH} \quad (1)$$

crystalline and pure form and in high yield, as previously observed for other similar compounds with the same environment.[18] Surprisingly, however, the crystal structure of (**1**) revealed (below) the configuration in this complex to be cis instead of trans. Nevertheless, the configuration observed in subsequent products obtained from the reactions of **1** with 4ptz ligands was always trans, proving cobalt(II) to be labile toward the rearrangement of the dbm ligands. Indeed, one of the goals in exploring the reactivity of [Co(dbm)$_2$(MeOH)$_2$] (**1**) with the polyfunctional ligand 4ptz was to investigate the possibility of the formation of a honeycomb 2D extended array, as expected from the combination of a trigonal knot (4ptz) and a potential linear linker such as **1**. Thus, complex **1** was allowed to react with 4ptz in THF solution in a 3:2 molar ratio, with the aim of replacing the axial groups on the metal with nitrogen donors of the multidentate ligand. To facilitate this, the process was conducted at the temperature of reflux, because the nitrogen-containing ligand is scarcely soluble in most solvents. At the end of the reaction, contrary to what was expected for the formation of a polymeric compound, no precipitate of a cobalt complex was obtained. Orange-red crystals could be obtained from Et$_2$O layers of the reaction system, which,

(3) Moulton, B.; Zaworotko, M. J. *Chem. Rev.* **2001**, *101*, 1629−1658.
(4) Gamez, P.; Reedijk, J. *Eur. J. Inorg. Chem.* **2006**, 29−42.
(5) Khlobystov, A. N.; Blake, A. J.; Champness, N. R.; Lemenovskii, D. A.; Majouga, A. G.; Zyk, N. V.; Schroder, M. *Coord. Chem. Rev.* **2001**, *222*, 155−192.
(6) Chen, B. L.; Liang, C. D.; Yang, J.; Contreras, D. S.; Clancy, Y. L.; Lobkovsky, E. B.; Yaghi, O. M.; Dai, S. *Angew. Chem., Int. Ed.* **2006**, *45*, 1390−1393.
(7) Halder, G. J.; Kepert, C. J.; Moubaraki, B.; Murray, K. S.; Cashion, J. D. *Science* **2002**, *298*, 1762−1765.
(8) Wu, C. D.; Hu, A.; Zhang, L.; Lin, W. B. *J. Am. Chem. Soc.* **2005**, *127*, 8940−8941.
(9) Quesada, M.; de Hoog, P.; Gamez, P.; Roubeau, O.; Aromi, G.; Donnadieu, B.; Massera, C.; Lutz, M.; Spek, A. L.; Reedijk, J. *Eur. J. Inorg. Chem.* **2006**, 1353−1361.
(10) Gamez, P.; de Hoog, P.; Roubeau, O.; Lutz, M.; Driessen, W. L.; Spek, A. L.; Reedijk, J. *Chem. Commun.* **2002**, 1488−1489.
(11) Quesada, M.; de la Peña-O'Shea, V. A.; Aromí, G.; Geremia, S.; Massera, M.; Roubeau, R.; Gamez, P.; Reedijk, J. *Adv. Mater.* **2007**, *19*, 1397−1402.
(12) Halder, G. J.; Neville, S. M.; Kepert, C. J. *Cryst. Eng. Comm.* **2005**, *7*, 266−268.
(13) Ohmori, O.; Kawano, M.; Fujita, M. *Cryst. Eng. Comm.* **2005**, *7*, 255−259.
(14) Dybtsev, D. N.; Chun, H.; Kim, K. *Chem. Commun.* **2004**, 1594−1595.
(15) Biradha, K.; Fujita, M. *Angew. Chem., Int. Ed.* **2002**, *41*, 3392−3395.
(16) Batten, S. R.; Hoskins, B. F.; Moubaraki, B.; Murray, K. S.; Robson, R. *Chem. Commun.* **2000**, 1095−1096.
(17) Kostyuk, N. N.; Shirokii, V. L.; Vinokurov, I. I.; Dik, T. A.; Umreiko, D. S.; Erdman, A. A. *Zh. Neorg. Khim.* **1992**, *37*, 68−71.
(18) Aromí, G.; Boldron, C.; Gamez, P.; Roubeau, O.; Kooijman, H.; Spek, A. L.; Stoeckli-Evans, H.; Ribas, J.; Reedijk, J. *Dalton Trans.* **2004**, 3586−3592.

instead of the expected honeycomb 2D array, were found by X-ray diffraction (XRD) (below) to correspond to the linear complex $[Co(dbm)_2(4ptz)]_n \cdot n$THF (**2a**), where one of the pyridyl rings of 4ptz was not engaged in coordination. The reason for the formation of **2a** instead of the coordinatively saturated complex predicted is to be found in the stabilization energy gained by the interactions between chains of **2a** observed in the solid state (below), which could not have taken place if the hexagonal network had formed. The same reaction performed in $CHCl_3$, on the other hand, produced significant amounts of an orange precipitate that was soluble in THF. Layers of this solution with $Et_2O$ led to the formation of red crystals of a compound (**2b**) that turned out to be a solvatomorph[19] of **2a** (below), displaying only very small conformational differences with the latter. Presumably, these differences are caused by slight changes in solvents of crystallization, because compound **2b** appears in the crystal as $[Co(dbm)_2(4ptz)]_n \cdot 0.75n$THF$\cdot 0.5n$Et$_2$O. A third isomorph, $[Co(dbm)_2(4ptz)]_n \cdot 3n$DMF (**2c**), was isolated as crystals directly from the reaction mixture, when the latter was performed in dimethylformamide (DMF). Compound **2c** again displays small differences from the supramolecular organization, which turned out to vary the magnetic properties significantly (below).

**Description of the Structures.** The structure of compounds **1**, **2a**, **2b**, and **2c** are presented in Figures 1−4. Crystallographic data for all of the complexes are collected in Table 1, whereas selected interatomic distances and angles are in Tables 2, 3, and 4 and in the caption of Figure 1.

**$[Co(dbm)_2(MeOH)_2]$ (1).** The structure of **1** (Figure 1) is described as a mononuclear molecule comprising one pseudo-octahedral cobalt(II) ion chelated by two $dbm^-$ ligands and two solvent MeOH molecules. Interatomic distances and angles featured by **1** are within normal ranges (caption of Figure 1). Surprisingly, these ligands are featured in cis configuration rather than trans. Of all of the mononuclear cobalt complexes containing only two 1,3-diketonate ligands (124 hits of the CCDC, version 5.27, Aug 2006), 51 are in cis configuration, of which the majority possess a third chelating ligand, the latter thus precluding the occurrence of the trans form. In fact, only about 15% of compounds of the type $[Co(1,3\text{-diketone})_2(L)_2]$ (L = monodentate ligand) are cis, and in these cases, there is usually a cause favoring this. In complex **1**, the reason for the rare cis conformation is the presence of self-complementary hydrogen bonding between molecules (Figure 1, bottom), where each MeOH ligand acts as a donor of a hydrogen bond to the oxygen atom of a dbm ligand from a neigbouring complex. Each molecule thus establishes a total of four such interactions, twice as a donor and twice as an acceptor, with two other molecules located on opposite sides, thereby forming chains of hydrogen-bonded complexes. The same situation was observed for a previously reported complex with a thienyl, trifluoromethyl-based 1,3-diketonate,[20] as is for the nickel analogue of **1** $[Ni(dbm)_2(MeOH)_2]$.[21] Besides this network of hydrogen bonds, no other intermolecular interactions other than weak van der Waals contacts occur within the crystal of complex **1**.

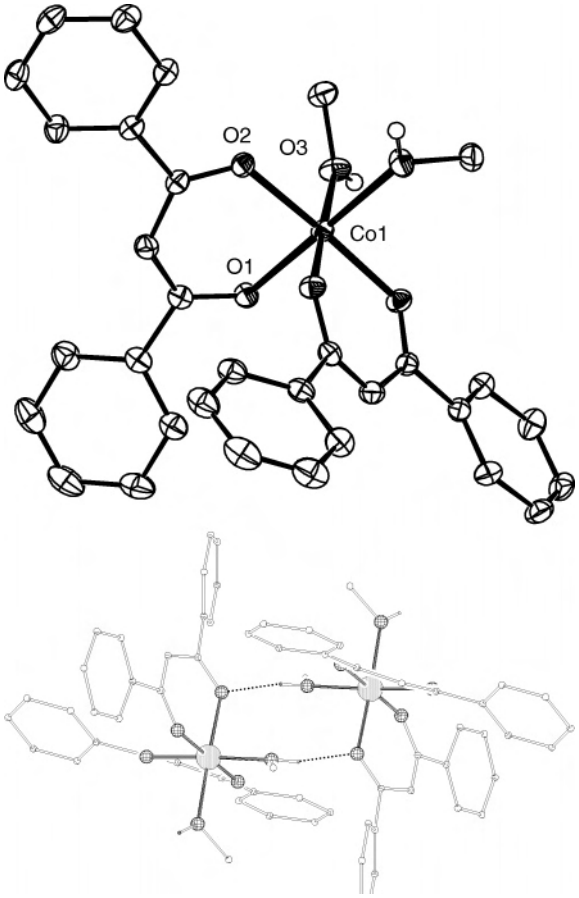


**Figure 1.** ORTEP representation (top) at the 50% probability level of complex $[Co(dbm)_2(MeOH)_2]$ (**1**). Unique atoms of the central chromophore are labeled. Only hydrogen atoms of the OH groups of the methanol ligands are shown. Selected bond distances (Å) and angles (°): Co(1)−O(1), 2.0589(14); Co(1)−O(2), 2.0242(14); Co(1)−O(3); 2.1134(14); O(1)−Co(1)−O(2), 89.20(5); O(1)−Co(1)−O(3), 91.83(5); O(1)−Co(1)−O(1)a, 90.43(5); O(1)−Co(1)−O(2)a, 88.85(5); O(1)−Co(1)−O(3)a, 177.72(5); O(2)−Co(1)−O(3), 90.84(5); O(2)−Co(1)−O(1)a, 88.85(5); O(2)−Co(1)−O(2)a, 177.22(6); O(2)−Co(1)−O(3)a, 91.19(5); O(3)−Co(1)−O(1)a, 177.72(5); O(3)−Co(1)−O(2)a, 91.19(5); O(3)−Co(1)−O(3)a, 85.92(5). 'a' represents the $[1 - x, y, {}^1/_2 - z]$ symmetry operation. Representation (bottom) of two molecules of **1**, emphasizing the self-complementary hydrogen bonding existing within chains of molecules in the crystal ([−O−H···O−], 2.799).

**$[Co(dbm)_2(4ptz)]_n \cdot n$THF (2a).** Compound **2a** is described as a linear coordination polymer resulting from the infinite succession of cobalt(II) ions and 4ptz ligands (part A of Figure 2). The metals constitute connection knots of 180° because their equatorial positions are saturated by two chelating dibenzoyl donors per center. The polydentate 4ptz ligands bridge pairs of metals through two of its pyridyl moieties, the third one remaining uncoordinated. The resulting system is therefore disposed in a zigzag configuration, with the uncoordinated pyridyl rings of the triazine-based ligands oriented outward. This favors the interdigitation of adjacent chains, allowing the establishment of a network of

(19) Chopra, D.; Row, T. N. G. *Cryst. Growth Des.* **2006**, *6*, 1267−1270.

(20) Pretorius, J. A.; Boeyens, J. C. A. *J. Inorg. Nucl. Chem.* **1978**, *40*, 1519−1528.

(21) Suzuki, H.; Matsumura, S.; Satoh, Y.; Sogoh, K.; Yasuda, H. *React. Funct. Polym.* **2004**, *59*, 253−266.

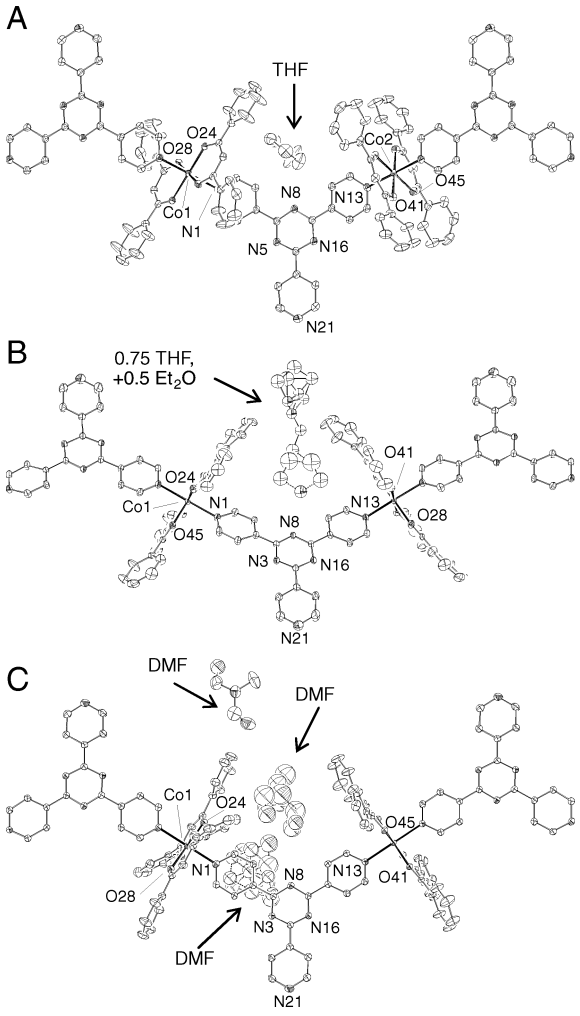


**Figure 2.** ORTEP representation at the 50% probability level of compounds [Co(dbm)$_2$(4ptz)]$_n$·*n*THF (**2a**, A), [Co(dbm)$_2$(4ptz)]$_n$·0.75*n*THF·0.5*n*Et$_2$O (**2b**, B), and [Co(dbm)$_2$(4ptz)]$_n$·3*n*DMF (**2c**, C). Hydrogen atoms are not shown for clarity. The amount of crystallization solvent per cobalt ion is shown.

$\pi-\pi$ interactions. Thus, each 4ptz ligand interacts with an equivalent partner located in front and slightly shifted, in such a way that the projection of one triazine nitrogen atom in one ligand falls near the center of the triazine ring opposite to it (part A of Figure 3). The distance between this nitrogen atom and the centroid of the triazine ring in front of it is 3.477 Å. The strain of the supramolecular organization in **2a** causes the 4ptz ligands to be significantly curved, instead of planar (part A of Figure 3, bottom), helping the chains to describe a sinusoidal line when observed from the side and along the zigzag plane (part A′ Figure 4). In these waves, the heterocyclic ligands lie at the maxima and minima of amplitude. Thus, each chain interacts with two parallel chains located on each side of the zigzag through two infinite sequences of 4ptz−4ptz interactions. Because each chain (wave) runs in opposite phase to the adjacent chain (Figure 4A′), the $\pi-\pi$ interactions occur between ligands located on points of opposite amplitude, thus, the interacting chains describe infinite sheets that are parallel to the zigzag planes (parts A and A″ of Figures 4). The space between sheets is efficiently occupied by the phenyl rings of the dbm$^-$ ligands and the molecules of tetrahydrofuran (THF). There are no additional $\pi-\pi$ stacking connections involving these rings. Therefore, it is very clear that the energy gain resulting from the interaction between 4ptz ligands is the main reason for the supramolecular disposition of the system in the solid state. The metals within the chains are separated by 13.143 Å, whereas the cobalt(II) ions of different chains can be as close as 8.632 Å.

Polymeric, structurally characterized complexes with the ligand 4-ptz as a $\mu$ bridge are very scarce in the literature.[22,23] The vast majority of coordination compounds made with this ligand have it in the $\mu_3$ mode, either as infinite arrays or as discrete, supramolecular architectures.[12−15]

**[Co(dbm)$_2$(4ptz)]$_n$·0.75*n*THF·0.5*n*Et$_2$O (2b).** The structure of **2b** (part B of Figure 2) reveals that the composition of this compound only differs from **2a** in the solvents of crystallization. Thus, **2b** also consists of a 1D polymer with alternating cobalt(II) ions and $\mu$-4ptz ligands in zigzag form, with the metals in the same coordination environment as in **2a**. However, in this compound there is one solvent site occupied by a molecule of THF with 50% occupancy, whereas a nearby site is occupied partially by either one molecule of Et$_2$O or one molecule of THF with 50 and 25% occupancies, respectively. These solvents occupy approximately the same position within the asymmetric unit as the THF molecule in **2a**; however, the differences cause a significant change in the supramolecular organization of the polymer in the crystal (Figures 3 and 4). Thus, whereas each chain is also interacting with two other chains on opposite sides through $\pi-\pi$ stacking of the 4ptz ligands (part B of Figure 4), the zigzag ribbons do not describe a sinusoidal conformation but show a rather flat disposition (part B′ of Figure 4). Thus, the adjacent interacting chains are located on top of each other and mutually shifted, describing infinite sheets in the form of a staircase (part C of Figure 4). The change in the spatial arrangement of the polymers cause the 4ptz−4ptz interactions to occur in a slightly different manner. In this case, the triazine rings are almost perfectly staggered (part B of Figure 3), forming quasi-ideal Piedfort pairs,[24,25] the distance between the centroids of the interacting triazine rings being 3.366 Å. The separation between adjacent metals within the chains is 13.292 Å, whereas the smallest interchain distance between two metals is 10.589 Å.

**[Co(dbm)$_2$(4ptz)]$_n$·3*n*DMF (2c).** Coordination complex **2c** (part C of Figure 2) shares the same composition as **2a** and **2b**, except for the solvents of crystallization, which now consist of three full molecules of DMF per asymmetric unit. These molecules are located in three well-defined areas within the unit cell but each of them displays more than one disordered orientation, as inferred by the inspection of part C of Figure 2. The new solvent composition results again in a different structural disposition of the zigzag polymers

(22) Rarig, R. S.; Zubieta, J. *J. Chem. Soc., Dalton Trans.* **2001**, 3446−3452.
(23) Cotton, F. A.; Lin, C.; Murillo, C. A. *J. Chem. Soc., Dalton Trans.* **2001**, 499−501.
(24) Piedfort pairs are pairs of 1,3,5-trisubstituted aromatic rings stacked in a perfectly staggered manner.
(25) Jessiman, A. S.; Macnicol, D. D.; Mallinson, P. R.; Vallance, I. *J. Chem. Soc., Chem. Commun.* **1990**, 1619−1621.

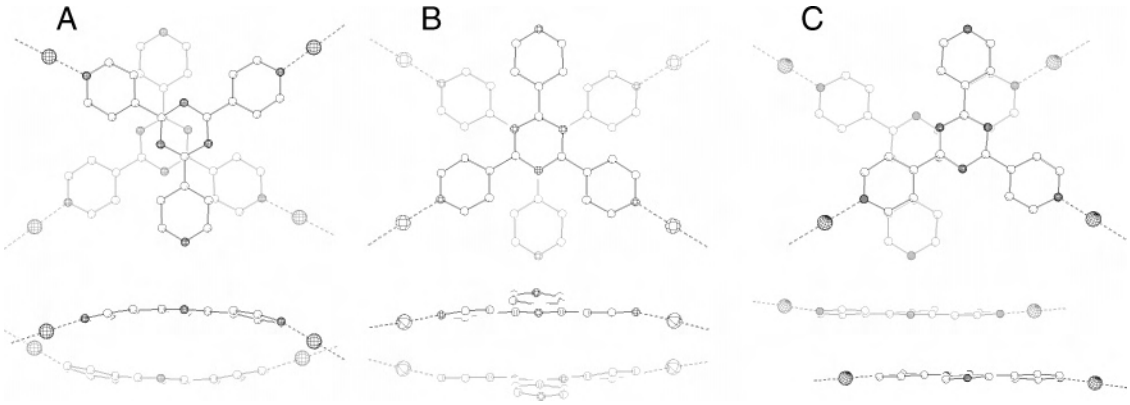


**Figure 3.** Two 4ptz ligands from adjacent chains of **2a** (A), **2b** (B), and **2c** (C) and the cobalt ions bound to them, emphasizing the $\pi-\pi$ stacking interactions existing between them. (Top) Top view. (Bottom) Side view.

throughout the lattice. In **2c**, each polymer interacts by interdigitation of the 4ptz ligands with two other equivalent polymers, one below and one above, as in **2b**. However, in the present compound, the ribbons are shifted with respect to each other along the 1D direction, by a distance of approximately the width of the triazine ring (~2.3 Å). Thus, the pairs of interacting 4ptz moieties do not project their triazine rings exactly on top of each other but in a shifted manner so that one triazine ring projects just next to the other (part C of Figure 3 and part C of Figure 4). The distance between the closest atoms from different triazine rings is 3.404 Å. The metals within the ribbons are located 13.280 Å apart, whereas the shortest Co···Co vector between chains is 9.979 Å long.

**Molecular Mechanics Calculations.** The structures of compounds **2a**, **2b**, and **2c** were surprising because it was expected that the most-favored outcome of the reactions leading to them would be the result of the maximum occupancy of the coordination sites of the 4ptz ligand. It was assumed that this would produce a 2D honeycomb architecture with fused hexagons featuring 4ptz ligands at the common edges and cobalt(II) knots on the sides (Figure 5), whereas the actual structure was completely different. This, in a way, could be taken as another argument in favor of a previously reported and rather provocative thought stating that "*One of the continuing scandals in the physical sciences is that it remains in general impossible to predict the structure of even the simplest crystalline solids from knowledge of their chemical composition*".[26] In this case, however, the composition of the expected product was also different from that which was finally isolated. It is very likely that the preference for linear chains (above) with one free coordination site on each 4ptz ligand is explained by the establishment of a network of $\pi-\pi$ interactions through interdigitation of these zigzag chains. The formation of a 2D honeycomb would prevent these interactions from taking place. To eliminate the hypothesis that there are steric reasons for the lack of formation of the 2D network, we performed molecular mechanics calculations. These were done with the program Gaussian 03, using the universal force field.[27] The results showed the hypothetical hexagonal polygon to be stable; therefore, there is not a steric reason for the prevention of its formation, thereby reinforcing the idea that the stacking interactions between the heterocycles are highly responsible for the supramolecular organization of compounds **2a**, **2b**, and **2c**. It is interesting to point out here that a recent report just appeared describing a coordination system that organizes as honeycombs at the supramolecular level, thanks to the establishment of $\pi-\pi$ interactions between the large-surface aromatic ligands composing it.[28]

**Magnetic Properties.** One of the driving forces for producing the assemblies reported here is the preparation of new magnetic materials. A study of the bulk magnetic properties was performed on complexes **2a** and **2c**. The interpretation of the magnetic behavior of octahedral cobalt(II) complexes is complicated by the spin−orbit coupling of the $^4T_{1g}$ ground state.[29] Calculation of exchange parameters can be done only for dinuclear complexes,[30,31] whereas full diagonalization methods allow for the determination of $J$ values for simple polynuclear systems in the low-temperature regions (where the effective spin $S'$ is $^1/_2$).[32] Complexes **2a** and **2c** are composed of 1D chains, and these can usually be considered as a succession of anisotropic $S = {}^1/_2$ pseudo spins of Ising type for their modeling.[33] Likewise, these systems are amenable to a phenomenological treatment (below).[34]

Bulk magnetization measurements of $[Co(dbm)_2(4ptz)]_n \cdot n$THF (**2a**) and $[Co(dbm)_2(4ptz)]_n \cdot 3n$DMF (**2c**) were performed in the 2−300 K range under a field of 5000 G and represented in the form of $\chi_M T$ versus $T$ plots (Figures 6 and 7), where $\chi_M$ is the molar paramagnetic susceptibility per cobalt(II). The $\chi_M T$ values at 300 K are (in the **2a**/**2c**

(26) Maddox, J. *Nature* **1988**, *335*, 201.

(27) Rappe, A. K.; Casewit, C. J.; Colwell, K. S.; Goddard, W. A.; Skiff, W. M. *J. Am. Chem. Soc.* **1992**, *114*, 10024−10035.

(28) Kammer, S.; Muller, H.; Grunwald, N.; Bellin, A.; Kelling, A.; Schilde, U.; Mickler, W.; Dosche, C.; Holdt, H. *Eur. J. Inorg. Chem.* **2006**, 1547−1551.

(29) Figgis, B. N.; Hitchman, M. A. *Ligand Field Theory and its Applications*; Wiley-VCH: New York, 2000.

(30) de Munno, G.; Julve, M.; Lloret, F.; Faus, J.; Caneschi, A. *J. Chem. Soc., Dalton Trans.* **1994**, 1175.

(31) Lines, M. E. *J. Chem. Phys.* **1971**, *55*, 2977.

(32) Borrás-Almenar, J. J.; Clemente-Juan, J. M.; Coronado, E.; Tsukerblat, B. S. *Inorg. Chem.* **1999**, *38*, 6081−6088.

(33) Angelov, S.; Drillon, M.; Zhecheva, E.; Stoyanova, R.; Belaiche, M.; Derory, A.; Herr, A. *Inorg. Chem.* **1992**, *31*, 1514−1517.

(34) Rueff, J. M.; Masciocchi, N.; Rabu, P.; Sironi, A.; Skoulios, A. *Eur. J. Inorg. Chem.* **2001**, 2843−2848.

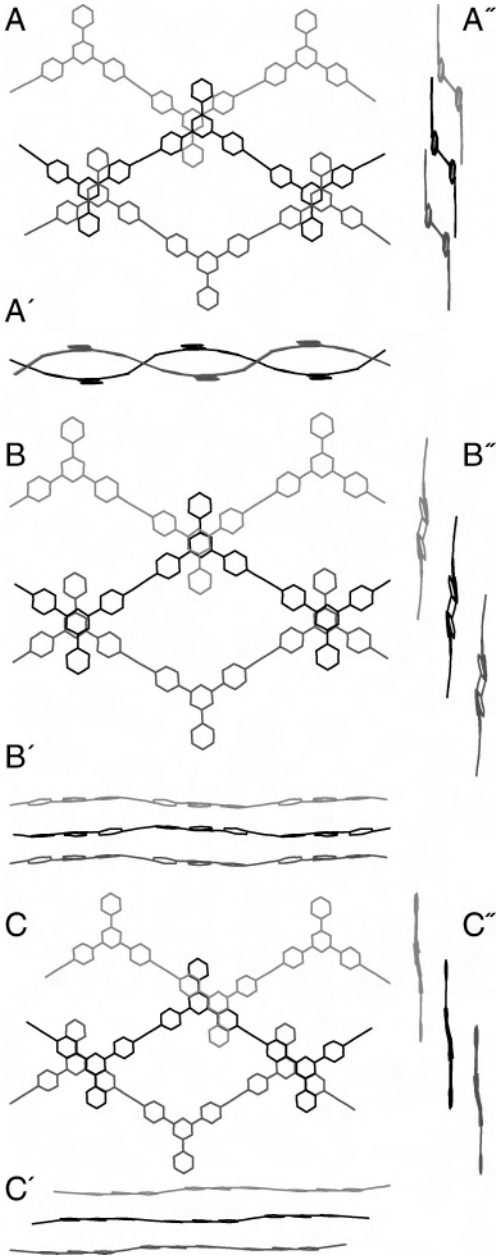


**Figure 4.** Stick representation of **2a** (top), **2b** (middle), and **2c** (bottom) emphasizing the supramolecular organization of the chains in the solid state. The dbm$^-$ ligands and solvate molecules are not shown for clarity, as well as the hydrogen atoms. (A, B, C) top view; (A′, B′, C′) side view perpendicular to the chains; (A″, B″, C″) side view parallel to the chains.

format) 3.7/3.4 cm$^3$ mol$^{-1}$ K, and these continuously decrease to 1.8/1.6 cm$^3$ mol$^{-1}$ K at 2 K. Spin−orbit coupling causes the observed 300 K $\chi_M T$ value to be higher than expected for an isolated $S = {}^3/_2$ system (1.87 cm$^3$ mol$^{-1}$ K) as well as its decrease upon cooling.[29,35] Values on the high end or above the range of 2.75−3.4 cm$^3$ mol$^{-1}$ K indicate very little deviation from ideal octahedral geometry. An estimation of the exchange interaction within such a 1D system can be obtained by using a two-exponential phenomenological equation (eq 2).[34]

In this equation, $A + B$ is equivalent to the Curie constant, $C$, whereas $E_1$ and $E_2$ represent the energies of the spin−orbit coupling and the exchange interaction, respectively. Excellent fits were obtained for both complexes with the following parameters (keeping the **2a**/**2c** format); $A + B =$ 3.7/3.6 cm$^3$mol$^{-1}$K, just above the range typically encountered for octahedral cobalt(II) ions ($C = \sim$2.8−3.4 cm$^3$ mol$^{-1}$ K),[34,36] $E_1/k$ = 103.9/86.3 cm$^{-1}$, of the same order as previously reported for analogous systems,[34,36] and for $E_2/k$ = 0.9/0.5 cm$^{-1}$ (i.e., $J = -1.8/-1.0$ cm$^{-1}$, using the Hamiltonian of the type $H = -JS_iS_j$ for the magnetic exchange). A temperature-independent paramagnetism value of 1.8 × 10$^{-3}$ cm$^3$ mol$^{-1}$ was employed for these fits, as is commonly done for octahedral cobalt(II) systems.[37] A small intrachain exchange interaction is not unexpected, given the extended nature of the bridge, formed by three heterocycles separated by single bonds. The reduced magnetization curve at 2 K, $M/N\beta$ versus $H/T$ tends to 2.5/2.2 $\mu_B$ at 2 T (not shown), in good agreement with the values reported in the literature.[34] More interesting about these compounds was the investigation into the possible magnetic exchange in two or three dimensions that could result from the supramolecular organization of the system in the solid state. This conjecture was investigated by examining the susceptibility of both compounds at various, lower magnetic fields or through ac measurements. Thus, when smaller magnetic fields were applied (20, 50, 100, 300, and 1000 G), $\chi_M T$ versus $T$ plots were obtained for compound **2a** that varied significantly with the magnitude of this field (Figure 6, inset). These plots were superimposable down to around 20 K and showed a moderate increase in the $\chi_M T$ value upon further cooling to reach maxima that were higher as the field became smaller. This is indicative of weak ferromagnetic ordering within the 3D network, which, in a system composed of antiferromagnetic chains, may originate as a result of the phenomenon of spin canting. This was further supported by results from ac measurements, which revealed $\chi_M''$ signals ($\chi_M''$ is the out-of-phase component of $\chi_M$) with maxima near 8 K, which were independent of the frequency used in the experiment (Figure S1 in the Supporting Information). Because the interactions within the 3D network leading to this canting are weak, the maxima of $\chi_M T$ versus $T$ do not reach very high values (4.13 cm$^3$ mol$^{-1}$ K under 20 G). The fact that the $M/N\beta$ versus $H/T$ curve does not increase rapidly at low fields corroborates that **2a** is not a ferromagnetic ordered solid. Moreover, no hysteresis response of the magnetization was observed at 2 K. The phenomenon of canting, which arises from single-ion magnetic anisotropy and/or antisymmetric interactions is relatively common, although the reported species with cobalt(II) are quite scarce. Some of them include the classical M[CoCl$_3$]$_n$ 1D systems,[38] a linear azido derivative,[39] or the hexameric complex (K$_2$[CoO$_3$PCH$_2$N(CH$_2$CO$_2$)$_2$])$_6$, the first discrete molecular system

(35) Telfer, S. G.; Sato, T.; Kuroda, R.; Lefebvre, J.; Leznoff, D. B. *Inorg. Chem.* **2004**, *43*, 421−429.

(36) Rueff, J. M.; Masciocchi, N.; Rabu, P.; Sironi, A.; Skoulios, A. *Chem.—Eur. J.* **2002**, *8*, 1813−1820.

(37) Boca, R. *Struct. Bonding* **2006**, *117*, 1−264.

(38) Carlin, R. L. *Magnetochemistry*; Springer: Berlin, Germany, 1986.

(39) Hong, C. S.; Koo, J. E.; Son, S. K.; Lee, Y. S.; Kim, Y. S.; Do, Y. *Chem.—Eur. J.* **2001**, *7*, 4243−4252.

**Table 1.** Crystallographic Parameters of Complexes **1**, **2a**, **2b**, and **2c**

| | **1** | **2a** | **2b** | **2c** |
|---|---|---|---|---|
| formula | $C_{32}H_{30}CoO_6$ | $C_{52}H_{42}CoN_6O_5$ | $C_{53}H_{45}CoN_6O_{5.25}$ | $C_{57}H_{55}CoN_9O_7$ |
| fw (g mol$^{-1}$) | 569.49 | 889.85 | 908.91 | 1037.03 |
| cryst syst | monoclinic | triclinic | monoclinic | triclinic |
| space group | *C*2/*c* | $P\bar{1}$ (no. 2) | $P2_1/n$ (no. 14) | $P\bar{1}$ (no. 2) |
| *a* (Å) | 16.9583(8) | 12.1547(5) | 10.5892(8) | 13.8982(11) |
| *b* (Å) | 16.3460(7) | 13.4488(5) | 26.548(2) | 14.1768(11) |
| *c* (Å) | 10.3880(6) | 15.7972(7) | 17.186 (1) | 15.0948(11) |
| α (deg) | 90.00 | 71.850(2) | 90.00 | 94.089(2) |
| *β* (deg) | 108.779(2) | 71.099(2) | 104.898(2) | 101.607(2) |
| *γ* (deg) | 90.00 | 70.895(2) | 90.00 | 112.116(2) |
| *V* (Å$^3$) | 2726.3(2) | 2246.7(2) | 4668.8(6) | 2663.3(4) |
| *Z* | 4 | 2 | 4 | 2 |
| $\rho_{calcd}$ (g cm$^{-3}$) | 1.388 | 1.315 | 1.293 | 1.293 |
| *T* (°C) | 150(2) | 150(2) | 150(2) | 150(2) |
| cryst shape | needle | block | parallelepiped | block |
| color | orange | red | red | red |
| dimensions (mm) | 0.40 × 0.08 × 0.08 | 0.27 × 0.12 × 0.12 | 0.30 × 0.30 × 0.17 | 0.06 × 0.03 × 0.01 |
| unique data | 3981 | 8741 | 9430 | 13 573 |
| unique data with $I > 2\sigma(I)$ | 2956 | 7365 | 8374 | 10 580 |
| R1, wR2[a] | 0.0410, 0.0988 | 0.0457, 0.1178 | 0.0659, 0.1824 | 0.0552, 0.1531 |

[a] $R1 = \sum||F_o| - |F_c||/\sum|F_o|$, $wR2 = [(\sum w(F_o^2 - F_c^2)^2 / \sum wF_o^4)]^{1/2}$.

**Table 2.** Selected Interatomic Distances (Angstroms) and Angles for Complex **2a**[a,b]

| | |
|---|---|
| Co(1)−O(24) | 2.0339(14) |
| Co(1)−O(28) | 2.0263(14) |
| Co(1)−N(1) | 2.2131(19) |
| Co(1)−O(24)a | 2.0339(14) |
| Co(1)−O(28)a | 2.0263(14) |
| Co(1)−N(1)a | 2.2131(18) |
| Co(2)−O(41) | 2.0360(16) |
| Co(2)−O(45) | 2.0347(16) |
| Co(2)−N(13) | 2.1603(17) |
| Co(2)−O(41)b | 2.0360(16) |
| Co(2)−O(45)b | 2.0347(16) |
| Co(2)−N(13)b | 2.1603(17) |
| Co(1)···Co(2) | 13.1427(6) |
| O(24)−Co(1)−O(28) | 91.12(6) |
| O(24)−Co(1)−N(1) | 89.52(6) |
| O(24)−Co(1)−O(24)a | 180.0 |
| O(24)−Co(1)−O(28)a | 88.88(6) |
| O(24)−Co(1)−N(1)a | 90.48(6) |
| O(28)−Co(1)−N(1) | 84.54(6) |
| O(28)−Co(1)−O(24)a | 88.88(6) |
| O(28)−Co(1)−O(28)a | 180.0 |
| O(28)−Co(1)−N(1)a | 95.46(6) |
| N(1)−Co(1)−O(24)a | 90.48(6) |
| N(1)−Co(1)−O(28)a | 95.46(6) |
| N(1)−Co(1)−N(1)a | 180.0000 |
| O(41)−Co(2)−O(45) | 90.44(6) |
| O(41)−Co(2)−N(13) | 91.32(6) |
| O(41)−Co(2)−O(41)b | 180.0 |
| O(41)−Co(2)−O(45)b | 89.56(6) |
| O(41)−Co(2)−N(13)b | 88.68(6) |
| O(45)−Co(2)−N(13) | 91.82(7) |
| O(45)−Co(2)−O(41)b | 89.56(6) |
| O(45)−Co(2)−O(45)b | 180.0000 |
| O(45)−Co(2)−N(13)b | 88.18(7) |
| N(13)−Co(2)−O(41)b | 88.68(6) |
| N(13)−Co(2)−O(45)b | 88.18(6) |
| N(13)−Co(2)−N(13)b | 180.0 |

[a] 'a' represents the [−*x*, 1 − *y*, 1 − *z*] symmetry operation. [b] 'b' represents the [$^3/_2 - x$, $^1/_2 + x$, $^1/_2 - x$] symmetry operation.

displaying this property at the solid state.[40] The canting in compound **2a** may be caused by the sinusoidal disposition of the chains of [−Co−4ptz−Co−4ptz−], which, together with the anisotropy of the cobalt(II) ions, leads to the generation of a net magnetization within the chain as a result of the antiferromagnetic ordering (Scheme 2). According to this, compound **2c** should not exhibit the phenomenon of canting, because the 1D ribbons in this compound are almost straight and not undulated (part C′ of Figure 4′). Indeed, the $\chi_M T$ versus *T* plots at different fields for **2c** are all superimposable, revealing the absence of canting. Likewise, this polymer showed no $\chi_M''$ signals in the ac magnetic measurements. This study demonstrates that solvents of crystallization may influence the supramolecular organization of MOFs, to the point of significantly changing their magnetic response.

**Table 3.** Selected Interatomic Distances (Angstroms) and Angles for Complex **2b**[a,b]

| | |
|---|---|
| Co(1)−O(24) | 2.026(2) |
| Co(1)−O(28)b | 2.0287(18) |
| Co(1)−O(41)b | 2.025(2) |
| Co(1)−O(45) | 2.0227(19) |
| Co(1)−N(1) | 2.189(2) |
| Co(1)−N(13)b | 2.214(2) |
| Co(1)···Co(1)b | 13.2920 |
| O(24)−Co(1)−O(28) | 89.08(7) |
| O(24)−Co(1)−O(41) | 178.71(8) |
| O(24)−Co(1)−O(45) | 91.49(8) |
| O(24)−Co(1)−N(1) | 94.15(8) |
| O(24)−Co(1)−N(13)b | 83.58(8) |
| O(28)−Co(1)−O(41) | 90.79(8) |
| O(28)−Co(1)−O(45) | 179.42(8) |
| O(28)−Co(1)−N(1) | 89.20(8) |
| O(28)−Co(1)−N(13)b | 91.73(8) |
| O(41)−Co(1)−O(45) | 88.64(8) |
| O(41)−Co(1)−N(1) | 84.57(8) |
| O(41)−Co(1)−N(13)b | 97.71(8) |
| O(45)−Co(1)−N(1) | 90.65(8) |
| O(45)−Co(1)−N(13)b | 88.44(8) |
| N(1)−Co(1)−N(13)b | 177.53(8) |

[a] 'a' represents the [−*x*, 1 − *y*, 1 − *z*] symmetry operation. [b] 'b' represents the [$^3/_2 - x$, $^1/_2 + x$, $^1/_2 - x$] symmetry operation.

## Experimental Section

**Syntheses.** All of the reactions were performed in air and using solvents and reagents as received.

(40) Gutschke, S. O. H.; Price, D. J.; Powell, A. K.; Wood, P. T. *Angew. Chem., Int. Ed.* **1999**, *38*, 1088−1090.

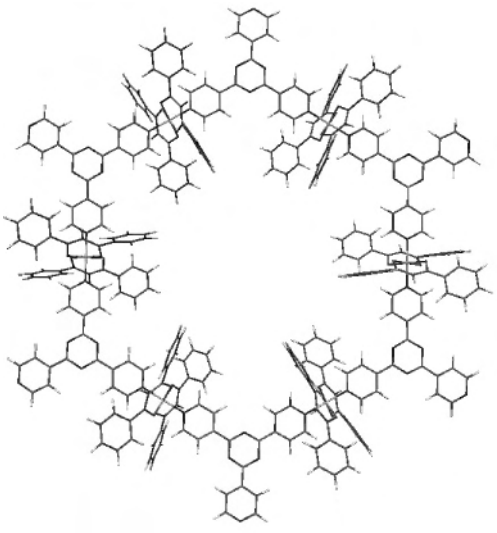

**Figure 5.** Representation of a structure with a hexagonal arrangement as calculated by molecular mechanics, showing that this architecture would be stable from the steric and electronic points of view.

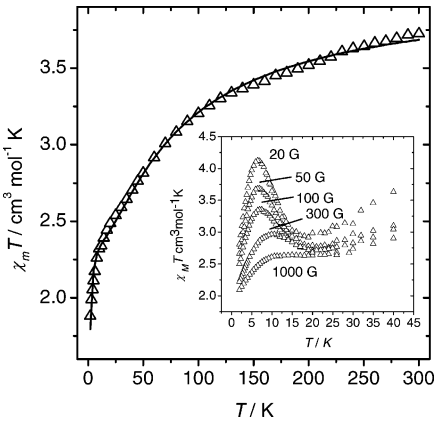


**Figure 6.** Plot of $\chi_M T$ versus $T$ per ion of cobalt(II) for [Co(dbm)$_2$(4ptz)]$_n$·$n$THF (**2a**) at a constant field of 5000 G. The solid line is a fit to the experimental data. The inset shows analogous plots of $\chi_M T$ versus $T$ at various fields.

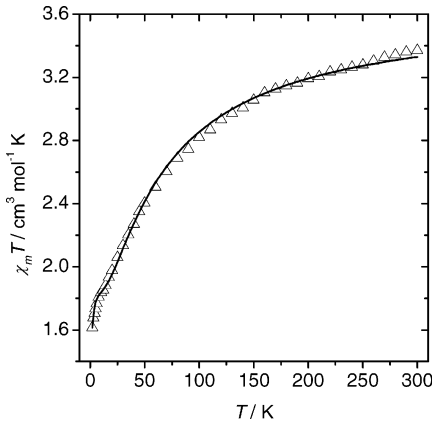


**Figure 7.** Plot of $\chi_M T$ versus $T$ per ion of cobalt(II) for [Co(dbm)$_2$(4ptz)]$_n$·3$n$DMF (**2c**) at a constant field of 5000 G. The solid line is a fit to the experimental data.

$$\chi_M T = A \exp(-E_1/kT) + B \exp(-E_2/kT) \qquad (2)$$

**2,4,6-Tris-(4-pyridyl)-1,3,5-triazine (4ptz).** This ligand was prepared through a slight modification of a published procedure.[41]

**Scheme 2.** Representation of the Sinusoidal [-Co-4ptz-Co-4ptz-] Chain of **2a** and the Possible Orientation of the Cobalt(II) Spin-Moments as a Result of the Antiferromagnetic Ordering of These and the Anisotropy of the Metal, to Yield a Nonzero Net Magnetization within the Chain

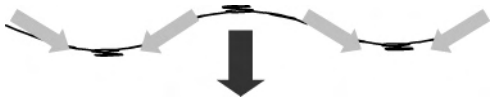

A mixture of 4-cyanopyridine (10 g, 96 mmol), 18-crown-6 (1 g, 3.8 mmol), potassium hydroxide (225 mg, 4.0 mmol), and decalin (10 mL) was stirred at near 200 °C for about 3 h. The system turned into a dark-brown solution upon warming. The solvents were distilled under a vacuum, and the residue, which consisted of a dark paste, was washed with warm pyridine and then with $Et_2O$. The product was obtained as pinkish crystals. The yield was 40%.

**[Co(dbm)$_2$(MeOH)$_2$] (1).** A yellow solution of dibenzoylmethane (Hdbm) (1.31 g, 5.3 mmol) in MeOH (80 mL) was added to a stirred magenta solution of $Co(AcO)_2 \cdot 4H_2O$ (0.73 g, 2.9 mmol) in MeOH (20 mL). The solution turned red-orange and an orange solid precipitated immediately. The mixture was kept undisturbed for 2 h at 4 °C, and then an orange product was collected by filtration, washed twice with $Et_2O$ (2 × 5 mL) after keeping the mother liquor, and dried in air. The yield was 62%. Anal. Calcd (Found) for **1**: C, 67.49 (67.17); H, 5.31 (5.04). Crystals suitable for X-ray crystallography were obtained from the mother liquor, after further slow evaporation. IR (cm$^{-1}$): 524.35 (*m*), 625.59 (*m*), 685.84 (*m*), 715.38 (*m*), 749.20 (*m*), 787.07 (*w*), 940.49 (*w*), 1023.06 (*m*), 1156.71 (*w*), 1230.15 (*m*), 1309.96 (*m*), 1395.66 (*vs*), 1453.53 (*s*), 1479.17 (*s*), 1523.04 (*vs*), 1547.79 (*s*), 1594.23 (*m*).

**[Co(dbm)$_2$(4ptz)]$_n$·$n$THF (2a).** Solid 4ptz (25 mg, 1.6 mmol) was added to a stirred orange solution of complex **1** (69 mg, 2.4 mmol) in tetrahydrofuran (THF) (25 mL). The orange mixture was brought to reflux, and the heating was maintained for 24 h, during which, the color turned to red-orange. After this, the resulting solution was allowed to cool to room temperature and was layered with $Et_2O$. After a few days, red, well-shaped crystals had formed on the walls of the tube. The yield was 60%. Anal. Calcd (Found) for **2a**: C, 70.19 (69.97); H, 4.76 (4.58); N, 9.44 (9.65). IR (cm$^{-1}$): 721.56 (*w*), 804.48 (*w*), 1062.58 (*w*), 1311.04 (*w*), 1371.95 (*m*), 1409.98 (*m*), 1456.79 (*s*), 1477.51 (*m*), 1520.59 (*vs*), 1549.22 (*m*), 1593.32 (*m*), 1616.63 (*m*).

**[Co(dbm)$_2$(4ptz)]$_n$·0.75$n$THF·0.5$n$Et$_2$O (2b).** Solid 4ptz (25 mg, 1.6 mmol) was added to a stirred orange solution of complex **1** (69 mg, 2.4 mmol) in $CHCl_3$ (25 mL). The mixture was stirred for 48 h, after which the color turned to red-orange, and an orange precipitate had formed. The solid was collected by filtration and washed three times with $Et_2O$ (3 × 5 mL). The orange solid was stirred with THF (10 mL) and layered with $Et_2O$. After a week, well-shaped red crystals had formed on the walls of the tubes, and a white microcrystalline product was found in suspension. The red crystals could be easily separated from the white material after successive washings with $Et_2O$. The yield was 20%. Anal. Calcd (Found) for **2b** (−0.5$n$Et$_2$O): C, 70.26 (70.10); H, 4.62 (4.76); N, 9.64 (9.40). IR (cm$^{-1}$): 690.96 (*w*), 722.83 (*w*), 802.30 (*w*), 1062.34 (*w*), 1312.10 (*w*), 1373.24 (*m*), 1412.05 (*m*), 1456.96 (*m*), 1478.08 (*m*), 1517.23 (*vs*), 1549.32 (*s*), 1593.12 (*m*).

**[Co(dbm)$_2$(4ptz)]$_n$·3$n$DMF (2c).** Solid 4ptz (25 mg, 1.6 mmol) was mixed with complex **1** (69 mg, 2.4 mmol) in DMF (30 mL) to yield a red-orange solution. The mixture was stirred for 2 h and

(41) Anderson, H. L.; Anderson, S.; Sanders, J. K. M. *J. Chem. Soc., Perkin Trans.* **1995**, 2231−2245.

was left to evaporate slowly. After three to four weeks, well-shaped red crystals had formed that were collected by filtration. The yield was 22%. Anal. Calcd (Found) for **2c**: C, 66.02 (65.72); H, 5.35 (5.20).; N, 12.16 (11.96). IR ($cm^{-1}$): 643.11 (*w*), 650.72 (*w*), 724.32 (*w*), 804.25 (*w*), 1062.17 (*w*), 1089.53 (*w*), 1222.91 (*w*), 1311.25 (*w*), 1372.92 (*s*), 1409.09 (*s*), 1457.89 (*s*), 1478.83 (*m*), 1517.16 (*vs*), 1548.58 (*vs*), 1592.43 (*m*), 1675.17 (*s*).

**Physical Measurements.** Field-cooled measurements of the magnetization of a smoothly powdered microcrystalline sample of **2a** were performed in the range of 2−300 K with a Quantum Design MPMS-5XL SQUID magnetometer with an applied field of 5 kG. Corrections for diamagnetic contributions of the sample holder to the measured magnetization and of the sample to the magnetic susceptibility were performed experimentally and by using Pascal's constants, respectively. Measurements were taken under an ac magnetic field in the 2−40 K range at 1339 and 107 Hz frequencies. IR spectra were recorded as KBr pellet samples on a Nicolet 5700 FTIR spectrometer. Elemental analyses were performed in-house on a Perkin-Elmer Series II CHNS/O Analyzer 2400, at the Servei de Microanàlisi of CSIC, Barcelona, Spain.

**X-ray Crystallography.** X-ray diffraction (XRD) data for compound **1** were recorded on a Nonius Kappa CCD diffractometer with graphite-monochromated Mo Kα radiation ($\lambda = 0.71073$ Å). DENZO-SMN was used for data integration, and SCALEPACK corrected data was used for Lorentz-polarization effects.[42] Measurements on single crystals of **2a**, **2b**, and **2c** were made using silicon-(111) monochromated synchrotron radiation ($\lambda = 0.8457$ Å) and a Bruker APEXII CCD area-detector diffractometer, using standard procedures and programs for Station 16.2 of Daresbury SRS. Data were collected on a Bruker APEXII diffractometer using the APEX2 software. In all three cases, the crystals were mounted onto the diffractometer at low temperature under nitrogen at ca. 150 K. The structures were solved using direct methods with the SIR92 (**1**),[43] SHELXTL (**2a**),[44,45] or SIR97 (**2b** and **2c**)[46] programs. Further refinements were done using the SHELXTL package. All of the non-hydrogens were refined anisotropically with the exception of disordered solvent areas in **2b** and **2c**; in the former, this area contains one molecule of $Et_2O$ (50% occupancy) and two THF molecules, which were disordered over two positions with 25 and 50% occupancies, respectively. Displacement parameters and 1,2/1,3 distance restraints were used to model these solvent molecules. A residual electron density peak remained in the refinement in the disordered solvent area that could not be modeled reasonably. Hydrogen atoms were placed geometrically on calculated positions on their riding atom. ($U$ij = 1.2 $U$eq for the atom to which they are bonded (1.5 for methyl)). For **2c**, the non-hydrogen atoms not refined anisotropically are those from solvents in disordered positions with less that 50% occupancy. In this compound, the hydrogen atoms placed in calculated positions were possible and refined using a riding model. In the case of the disordered DMFs, it was not possible to either place or find them in the difference map, and they were omitted from the refinement. Geometrical and displacement parameter restraints were used to model the disordered DMF. Displacement parameter restraints were used in the modeling of one of the phenyl rings, and even so, a couple of carbon atoms have displacement parameter ratios max/min of around 5:1. Splitting the cited was considered, but as no new chemical information would result, they were left as they were.

## Conclusions

Intermolecular hydrogen-bonding interactions are at the root of the unexpected cis configuration displayed by the complex $[Co(dbm)_2(MeOH)_2]$ (**1**) in the solid state, as revealed in this work by single-crystal X-ray crystallography. This configuration rearranges into trans upon reaction with the multidentate, radial 4ptz ligand. The resulting product is a 1D polymer of the formula $[Co(dbm)_2(4ptz)]_n$, with a zigzag arrangement instead of the expected honeycomb organization, despite the fact that molecular mechanics calculations demonstrate that such architecture would be stable. The reason for the observed solid-state structure is the establishment of a network of $\pi-\pi$ stacking interactions, which represent a higher energy gain than full coordination of the 4ptz ligand. Three isomers of this polymer have been prepared and characterized by single-crystal XRD, which differ in the nature and position of crystallization solvents and result in different relative dispositions of the 1D chains at the supramolecular level. A study of the magnetic properties of two of the polymers reveals that the supramolecular structure has a profound impact on the magnetic properties of the solid. Thus, the compound where the 1D chains exhibit a sinusoidal shape (**2a**) shows the phenomenon of spin canting, presumably as a consequence of the mutually tilted orientation of the cobalt(II) centers within the chains. If the chains are straight (**2b** and **2c**), the spin canting disappears. This opens the prospect of exploiting derivatives of this new type of system for the investigation of spin canting as a function of various subtle structural factors.

**Acknowledgment.** This work was supported by Dutch WFMO (Werkgroep Fundamenteel-Materialen Onderzoek), CW (Foundation for the Chemical Sciences), and NWO (Organization for the Scientific Research), the CNRS, Bordeaux 1 university, and the Spanish Ministerio de Ciencia y Tecnología through a "Ramón y Cajal" contract. We acknowledge the provision of time at the CCLRC Daresbury Laboratory via support by the European Union.

**Supporting Information Available:** X-ray crystallographic data in CIF format. This material is available free of charge via the Internet at http://pubs.acs.org.

IC7004979

(42) Otwinowski, Z.; Minor, W. *Methods Enzymol.* **1996**, *276*, 307.
(43) Altomare, A.; Cascarano, G. G.; Giacovazzo, C.; Guagliardi, A.; Burla, M. C.; Polidori, G.; Camalli, M. *J. Appl. Crystallogr.* **1993**, *27*, 435.
(44) Sheldrick, G. M.: University of Göttingen, 1997.
(45) Sheldrick, G. M.: University of Göttingen, 1997.
(46) Altomare, A.; Burla, M. C.; Camalli, M.; Cascarano, G. L.; Giacovazzo, C.; Guagliardi, A.; Moliterni, A. G. G.; Polidori, G.; Spagna, R. *J. Appl. Crystallogr.* **1999**, *32*, 115−119.